# Colour Analysis of Inland Waters Using Landsat TM Data

**J.-M. Jaquet**
*Dept. of Geology, University, 13 rue des Maraîchers, CH-1211 Geneva*

**B. Zand**
*GRID-Processor, UNEP, 8 rue de la Gabelle, CH-1227 Geneva*

*Chromaticity transforms based on TM bands 1, 2 and 3 have been computed for over 50 inland water bodies located in western Switzerland and south-eastern France. They include large, deep subalpine lakes, Jura and alpine mountain lakes, reservoirs, ponds and rivers. Their trophic state varies between oligotrophic and eutrophic.*

*In chromaticity space, hue range from green-blue, moderately saturated (clear water) to green, less saturated (high chlorophyll). A third pole is located towards isoradiance point (high mineral turbidity). Targets with bottom signal influence plot in between.*

*It is shown that colour transforms yield more information on water bodies typology and features than principal component analysis based on band radiances.*

Keywords: Landsat, TM, inland waters, chromaticity, water colour, classification

## 1. Introduction

The classification of water into 'types', based on optical properties (Jerlov 1976), has been widely applied to oceans. Colour studies of sea water were given a significant impetus by the advent of Nimbus CZCS, and numerous algorithms are now available to link the spectral signature of water to its chlorophyll or suspended solid content.

The relatively small size of many inland water bodies has not favoured the use of CZCS in limnology. To date, most of the applications of remote sensing to coastal or inland waters studies have been based on Landsat MSS data. The approaches taken are:

1) *Classifying water bodies on the basis* of multiband intensity data into types related to the trophic spectrum (oligotrophic to eutrophic). Examples include the work of Wezernak et al. (1976), Blackwell and Boland (1976), Lillesand et al. (1983) and McGarrigle and Reardon (1986).
2) *Statistically relating single-band intensities* (as DN values) *or band ratio* to usual limnological parameters such as turbidity (Piech et al. 1978, Shimoda et al. 1984, Lindell et al. 1985), Secchi depth SD (Smith and Addington 1978), or chlorophyll (Lemoalle 1979).
3) *Computing water colour by chromaticity analysis* and relating chromaticity coordinates to turbidity and other water quality parameters (Alfoldi and Munday 1978, Munday et al. 1979). The MSS of Landsat being devoid of a blue band, this transform results in a 'false colour' description: the information from intensity is eliminated, leaving only hue and saturation.

The advent of the Thematic Mapper affords the limnologist the following a priori advantages over MSS:
(i) presence of a near-blue band;
(ii) better spatial resolution (30 m vs. 80 m);
(iii) availability of a thermal IR band.

According to Tassan (1984), the chlorophyll and sediment (sm) retrieval performance of TM approximately matches that of CZCS in marine situations (where sm is correlated to chlorophyll). So far, only a few applications of TM to limnology have been published (see for example Lathrop and Lillesand 1986, 1987).
Taking advantage of these features, we present here (a) a colour analysis of inland water bodies, (b) compare it with the results of a classical unsupervised classification and (c) relate it to known limnological paramaters such as trophic status, bottom effects, and presence of submerged aquatic vegetation (SAV).

To keep variability sources to a minimum, the analysis was conducted on a single date and a single frame. Work

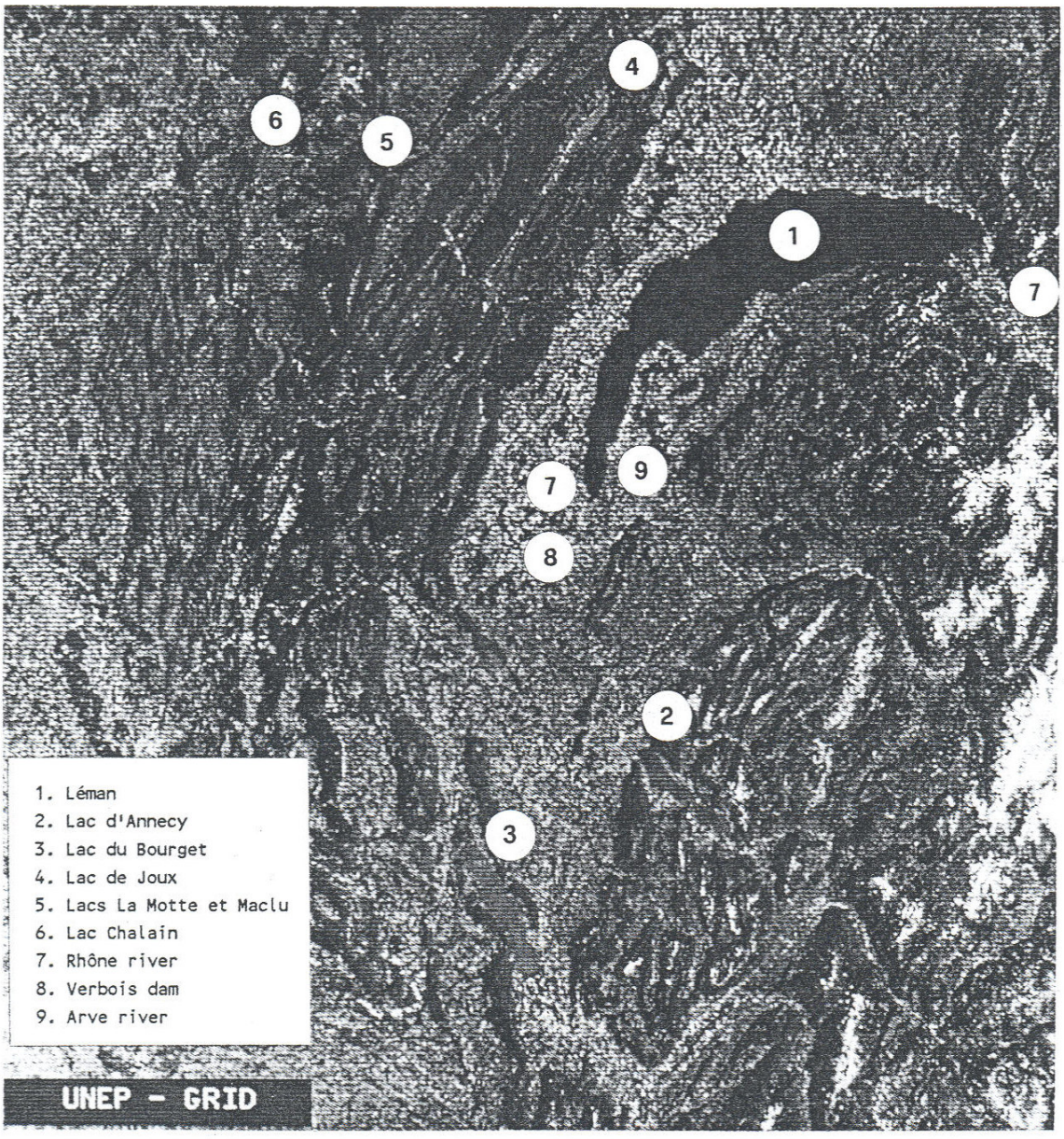


*Figure 1. True colour image of Landsat TM frame 196/028 (30.07.84) showing some of the water bodies mentioned in the text. Length of Léman is approximately 100 km.*

is in progress to extend it to a broader scale, temporally and geographically.

## 2. Material and Methods

### 2.1. Scene

Within the framework of the TM Pilot Studies, three adjacent frames were provided by ESA/Earthnet through the Swiss NPOC: 195/028, 196/027 and 196/028. Only the last one, taken on 30 July 1984, will be considered here. The Earthnet acquisition station is Fucino, and the data are system-corrected (radiometric preflight and geometric correction). There is no cloud cover and the visibility vote equals 3.

Frame 196/028 covers the Jura mountains, the Plateau and part of the Alps in Western Switzerland and SE France (Fig. 1). Over 50 water bodies ranging in size from the large, deep subalpine lakes (Léman, Annecy, Bourget) to small Jura or alpine lakes or rivers have been studied. The span of their trophic status is rather large, and they are either natural or man-controlled.

### 2.2. Image handling and calculations

Polygons were drawn (a) at the limit between land and water by displaying band-4 images, thus including the

**Table 1 - LANDSAT-5 TM RADIANCE CONVERSION PARAMETERS FOR SCENE 196/028 (30.07.84)**

| Band | Spread Min | Spread Max | A0 | A1 |
|---|---|---|---|---|
| 1 | 45 | 255 | -.067 | .042 |
| | | | -.117 | .064 |
| 2 | 1 | 255 | -.157 | .104 |
| | | | -.215 | .127 |
| 3 | 10 | 255 | -.113 | .065 |
| | | | -.185 | .098 |
| 4 | 6 | 255 | -.233 | .117 |
| | | | -.207 | .092 |
| 5 | 2 | 255 | -.086 | .027 |
| | | | -.042 | .013 |
| 7 | 1 | 255 | -.051 | .017 |
| | | | -.022 | .007 |

A0: mW cm-2 sr-1 µm-1 A1: mW cm-2 sr-1 µm-1 DN-1

For each band:: first line = in-flight values
2nd line = preflight values
(SLATER et al. 1987)

whole water body (labelled Zbat=0 in Table 2) and (b) between inshore and pelagic zones (depth greater than 5-10 m depending on the water body; Zbat=P). This was done on the basis of bathymetric charts when available (Delebecque 1898 and large-scale Swiss and French topo maps), or by exclusion of areas with obvious bottom signal (see Fig. 2a). In some instances, they were specifically sampled and are labelled Zbat=F in Table 2.

Band statistics were computed for each polygon and chromaticity values calculated after transformation of the DN's into radiance $Li$ (mW.cm$^2$.sr.$\mu$m) by means of the $A0$ and $A1$ coefficients found in the CCT radiometric calibration ancillary record (Table 1). The formulae are:

$$X = L1/\Sigma Li, \quad Y = L2/\Sigma Li \quad \text{and } Z = L3/\Sigma Li.$$

Initially, an approximate atmospheric correction was applied to the data by 'dark pixel subtraction' (Rochon 1975). Since all the shadows used for correction were on land, the subtracted radiance would be too high (Piech and Walker 1971) and result in some negative values for water. Pending the application of a formal atmospheric correction, chromaticities were computed on uncorrected radiances. This does not affect the relative position of water bodies in the $XYZ$ chromaticity space, but shifts them all towards the blue pole.

To preserve spatial resolution which is a prerequisite for the study of small lakes and narrow rivers, no filtering was applied to eliminate the various banding types present in the data (Poros and Peteron 1985). However, an estimate of total variability due to various noise sources was obtained by computing band coefficient of variation for a seemingly homogeneous area (250×250 pixels) in Lac Léman (Fig. 1) with the following results: band 1: 2.1%; band 2: 3.0%; band 3: 5.1% and band 4: 6.7%. The differences in odd and even 16-line band mean values were 0.3, 0.5, 1.5 and 5% respectively. As a rule, we considered that differences between water bodies in terms of DN's had to be >10% to be considered as significant.

Data handling and image processing were done at the GRID-processor in Geneva using ELAS and ERDAS systems. Multiband classification of water bodies was performed on principal component scores by the modules PRINCE and CLUSTR (ERDAS). This last system was also applied when digitising bathymetric maps and setting up a GIS, in order to superimpose contours over satellite imagery (Fig. 2).

## 3. Results

### 3.1. Penetration depth of imagery

In order to assess the true signal from lake water, the influence of bottom reflection must be eliminated. According to Gordon and McCluney (1975), the penetration depth $Z90 < 1/a$, where $a$ is the absorption coefficient of water for given wavelength. Since the values of $a$ are not available for our dataset, a safe estimate of maximum penetration depth can be computed from Scherz and Van Domelen's (1974) Figure 5, whereby Z90max < SD for white light (see also Jaquet 1987).

From the population of water bodies listed in Table 2, we have selected clear lakes La Motte and Maclu (Fig. 1), which have a rather low reflectance in each band and white chalk banks along their western shore (Fig. 2). In band 1, the bottom signal is perceived approximately down to the 10 m contour. This value is close to the maximum SD readings known in these lakes (Verneaux et al. 1987). It is therefore safe to use Z90=10 m as a maximum penetration depth or limit for the pelagic zone, since all the other lakes studied have SD < 10 m, or bottom less reflective than chalk.

### 3.2. Colour analysis

*3.2.1. Poles and loci*

The various water targets considered are plotted on colour diagrams shown in Figure 3, both as $XY$ and triangular diagrams. Owing to the position and width of the TM bands, chromaticity coordinates do not represent 'pure' blue, green or red, but rather blue-green centered at 480 nm ($X$), green-yellow centered at 560 nm ($Y$) and red centered at 650 nm ($Z$). It should also be kept in mind that the swarm of points represent radiances not corrected for atmospheric influence.

**Table 2 - LIST AND CHARACTERISTICS OF WATER BODIES IN SCENE 196/028 (30.07.84)**

| Name | No | Surf | Locat | Alt | Trop | Type | Zbat |
|---|---|---|---|---|---|---|---|
| CHALAIN_0 | 1 | 2435 | JURA | 488 | | N | 0 |
| CHALAIN_5 | 2 | 1509 | JURA | 488 | | N | P |
| NARLAY_P | 3 | 132 | JURA | 748 | | N | P |
| GD_MACLU_P | 4 | 72 | JURA | 775 | O | N | P |
| LA_MOTTE_P | 6 | 244 | JURA | 774 | O | N | P |
| CHAMBLY_NP | 7 | 65 | JURA | 500 | | N | P |
| CHAMBLY_SP | 8 | 119 | JURA | 500 | | N | P |
| BONLIEU_P | 9 | 61 | JURA | 790 | | N | P |
| MOTTE_1 | 96 | 14 | JURA | 774 | | F | |
| ABBAYE_P | 10 | 190 | JURA | 871 | | N | P |
| CLAIRV_NO | 11 | 588 | JURA | 525 | | N | 0 |
| CLAIRV_NP | 12 | 239 | JURA | 525 | | N | P |
| CLAIRV_SP | 13 | 84 | JURA | 525 | | N | P |
| ROUSSES_P | 14 | 196 | JURA | 1058 | | N | P |
| JOUX_0 | 15 | 8959 | JURA | 1004 | | N | 0 |
| JOUX_P | 16 | 5227 | JURA | 1004 | E | N | P |
| TER | 17 | 15 | JURA | 1030 | | N | P |
| BRENET_P | 24 | 371 | JURA | 1002 | E | A | P |
| BRENET_0 | 25 | 616 | JURA | 1002 | | A | 0 |
| ANNECY_0 | 26 | 27582 | ALPES | 445 | O | N | 0 |
| ANNECY_P | 27 | 1863 | ALPES | 445 | | N | P |
| GIROTTE_P | 28 | 404 | ALPES | 1730 | | A | P |
| GITTAZ_P | 29 | 128 | ALPES | 1562 | | A | P |
| ROSELEND_0 | 30 | 2858 | ALPES | 1553 | | A | 0 |
| ROSELEND_P | 31 | 1282 | ALPES | 1553 | | A | P |
| GUERIN_P | 32 | 123 | ALPES | 1557 | | N | P |
| BOURGET_0 | 33 | 44324 | PLATEAU | 230 | | N | 0 |
| BOURGET_P | 34 | 2688 | PLATEAU | 230 | M | N | P |
| AIGUEBEL_0 | 35 | 5787 | JURA | 373 | | N | 0 |
| AIGUEBEL_P | 36 | 2380 | JURA | 373 | | N | P |
| VOUGLANS_S | 37 | 2684 | JURA | 350 | | A | P |
| VOUGLANS_M | 38 | 4370 | JURA | 350 | | A | P |
| VOUGLANS_N | 39 | 774 | JURA | 350 | | A | P |
| CONDES_P | 40 | 1468 | JURA | 308 | | A | P |
| NANTUA_0 | 41 | 1413 | JURA | 475 | | N | 0 |
| NANTUA_P | 42 | 857 | JURA | 475 | E | N | P |
| SYLANS_P | 43 | 135 | JURA | 580 | | N | P |
| REMORAY_CR | 44 | 81 | JURA | 851 | | F | |
| REMORAY_0 | 45 | 1080 | JURA | 851 | | N | 0 |
| REMORAY_P | 46 | 466 | JURA | 851 | | N | P |
| GRUYERES_P | 47 | 1216 | PLATEAU | 677 | | A | P |
| MONTSALVEN | 48 | 132 | ALPES | 801 | | A | P |
| SARINE_P | 49 | 116 | ALPES | 900 | | ? | P |
| BRET_P | 52 | 145 | PLATEAU | 674 | E | A | P |
| BRET_0 | 53 | 466 | PLATEAU | 674 | | A | 0 |
| EMOSSON | 54 | 1639 | ALPES | 1930 | | A | P |
| SALANFE | 55 | 1006 | ALPES | 1925 | | A | P |
| MONTRION_P | 56 | 102 | ALPES | 1070 | | N | P |
| ANTERNE_P | 57 | 53 | ALPES | 2060 | O | N | P |
| NOIR | 58 | 26 | ALPES | 1947 | O | N | P |
| DIVONNE_P | 59 | 142 | PLATEAU | 460 | | A | P |
| VERBOIS | 60 | 165 | PLATEAU | 372 | | A | P |
| MACHILLY_P | 61 | 36 | PLATEAU | 520 | E | N | P |
| LEMAN_P | 62 | 548517 | PLATEAU | 372 | M | N | P |
| LEMAN_VIDY | 63 | 6926 | PLATEAU | 372 | | Z | P |
| LEMAN_ROLL | 64 | 6129 | PLATEAU | 372 | | Z | P |
| LEMAN_DRAN | 65 | 3005 | PLATEAU | 372 | | Z | P |
| LEMAN_EVIA | 66 | 4262 | PLATEAU | 372 | | Z | P |
| LEMAN_LOCU | 67 | 1525 | PLATEAU | 372 | | Z | P |
| LEMAN_RHON | 68 | 4746 | PLATEAU | 372 | | Z | P |
| LEMAN_VILL | 69 | 4491 | PLATEAU | 372 | | Z | P |
| ARVE_MIN | 70 | 0 | PLATEAU | 370 | | R | P |
| ARVE_CONTA | 71 | 0 | PLATEAU | 370 | | R | 0 |
| RHONEVS_A | 72 | 0 | ALPES | 372 | | R | P |
| RHONEVS_B | 73 | 0 | ALPES | 372 | | R | P |
| RHONE_GEA | 74 | 0 | PLATEAU | 374 | | R | P |
| TANNAY_P | 77 | 39 | ALPES | 1408 | O | N | P |
| HONGRIN_P | 78 | 673 | ALPES | 1255 | | A | P |
| GENIN | 79 | 19 | JURA | 836 | | N | P |
| PALEXPO | 80 | 21 | PLATEAU | 440 | | T | |
| RHONE_BUTI | 81 | 22 | PLATEAU | 370 | | R | P |
| RADE_GE | 82 | 86 | PLATEAU | 372 | | Z | P |
| ARVE_BATIE | 83 | 22 | PLATEAU | 370 | | R | P |
| LEM_VENG | 84 | 140 | PLATEAU | 373 | | F | |
| LEM_BIT | 85 | 40 | PLATEAU | 373 | | F | |
| LEM_TRAVER | 86 | 32 | PLATEAU | 372 | | F | |
| LEM_BABYPL | 87 | 98 | PLATEAU | 372 | | F | |
| LEM_NAUTIQ | 88 | 29 | PLATEAU | 372 | | F | |
| LEM_GRANG1 | 89 | 160 | PLATEAU | 372 | | F | |
| LEM_GRAN2 | 90 | 120 | PLATEAU | 372 | | F | |
| LEM_GRAN3 | 91 | 306 | PLATEAU | 373 | | F | |
| CLAIRV_1 | 93 | 21 | JURA | 525 | | F | |
| CLAIRV_2 | 94 | 33 | JURA | 525 | | F | |
| CLAIRV_3 | 95 | 35 | JURA | 525 | | F | |

Surface: in pixels
Altitude: in m.
Localisation: natural region
Trophic state: Eutro, Meso, Oligotrophic
Type: Natural, Artificial, Zone within lake, F = bottom, T = roof, River
Zbat: 0 = whole lake, Pelagic (>10m)

On the triangular diagram of Figure 3a, the water bodies are located approximately between green-blue (GB) and green radii (hue dimension), with saturation ranging from 20 to 50% (Alföldi and Munday 1978). A light-grey roof top used as reference is located at T.

A subset of the water bodies is plotted on Figure 4. Symbols illustrate the a priori typology of the targets (lakes, rivers, bottom, etc.) and lines represent typical sequences or loci. By this term, we mean a natural sequence of water bodies, either following bathymetry or along a tur-

*Figure 2. Influence of bottom signal from Chalk Banks in TM bands 1 (strong) and 4 (weak) for lakes La Motte and Maclu.*

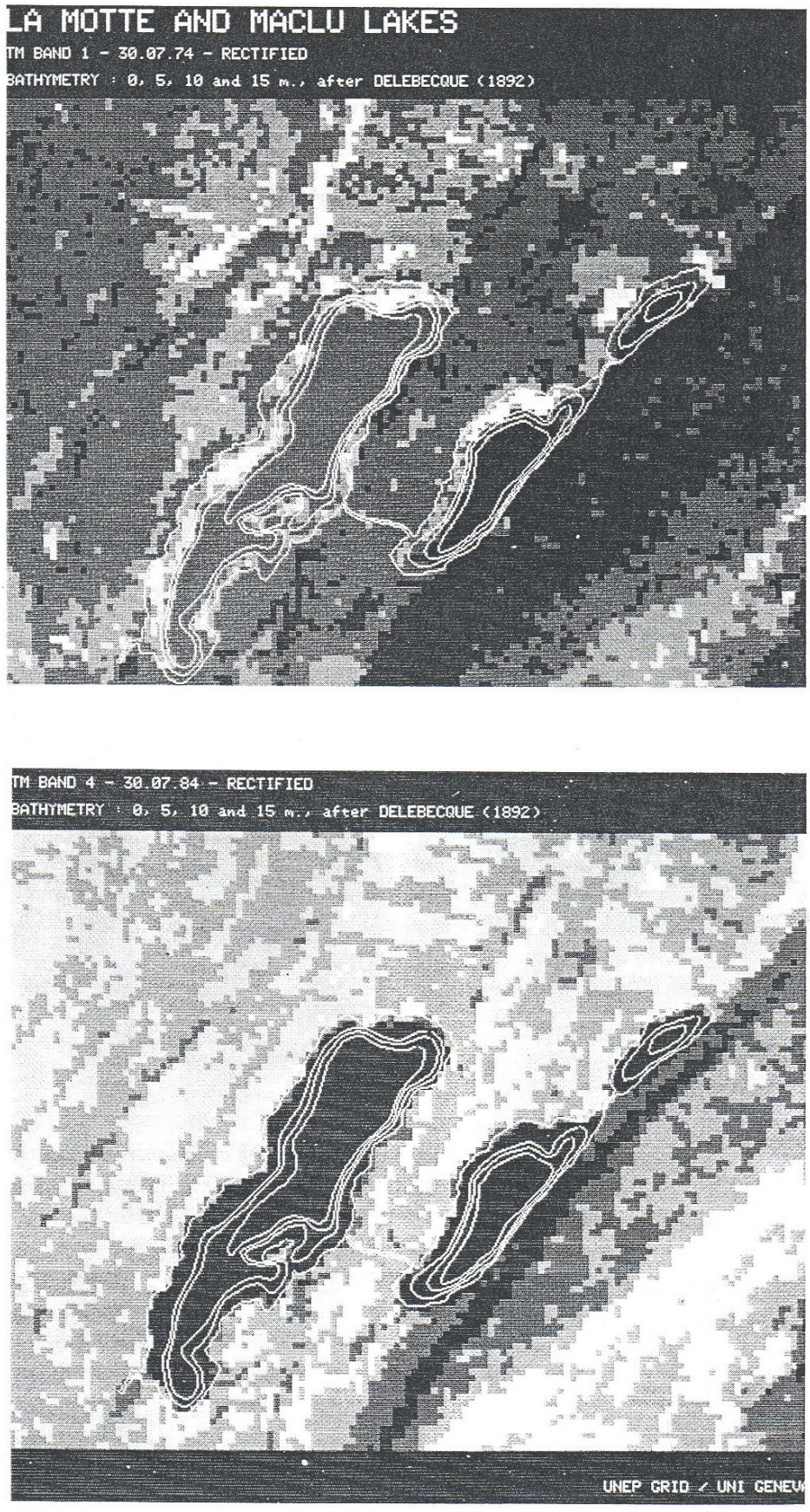

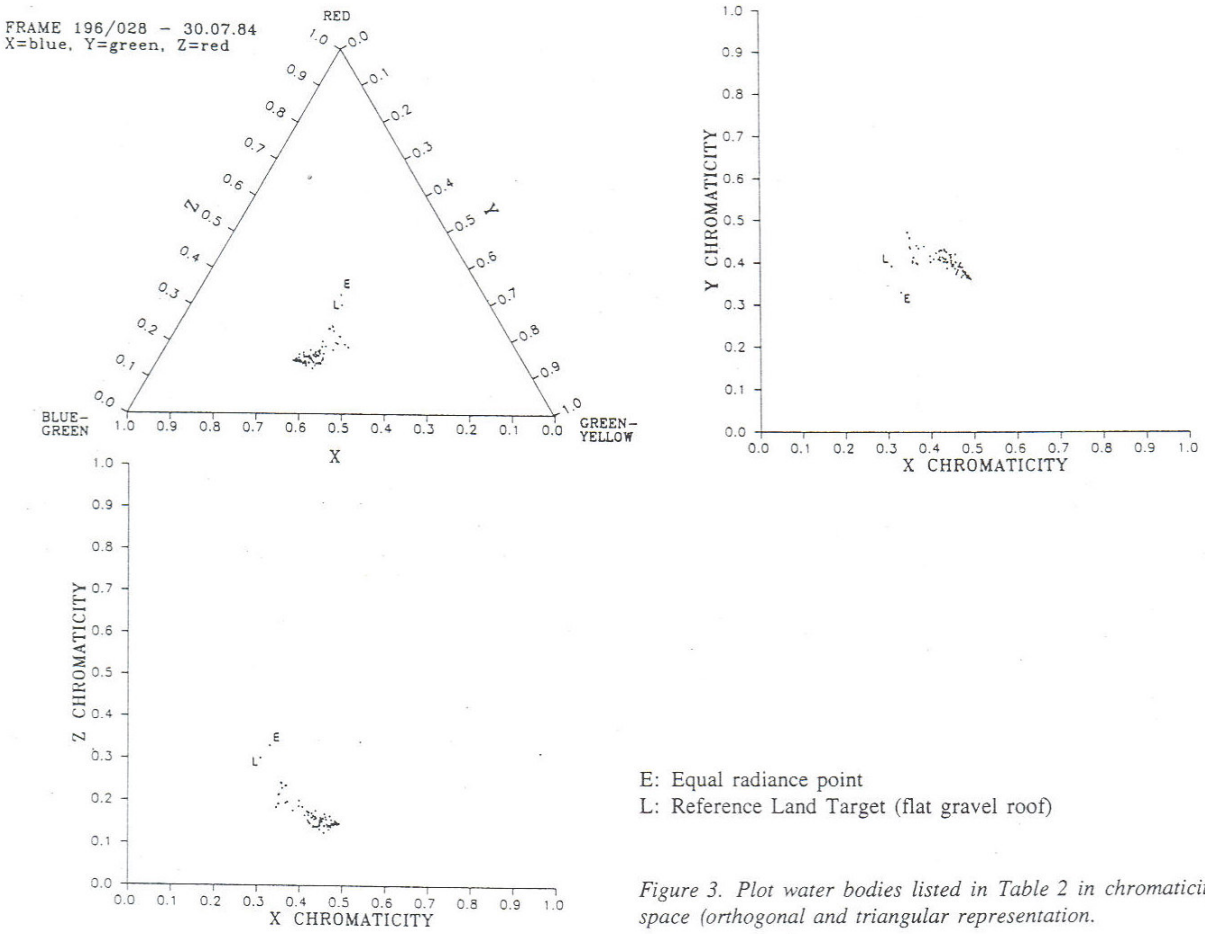


E: Equal radiance point
L: Reference Land Target (flat gravel roof)

*Figure 3. Plot water bodies listed in Table 2 in chromaticity space (orthogonal and triangular representation.*

bidity gradient. These loci generally point towards a few attraction points (AP) also shown on the diagrams.

The water bodies located at maximum $X$ values represent the clearest lakes of our dataset, seen as green-blue from the satellite (W). The pole of clearest known lake water would be at higher saturation towards the blue (Crater lake, Smith et al. 1973).

A second AP (C), located at maximum $Y$ values is occupied by eutrophic lac de Joux and lac Brenet, characterised by high chlorophyll content and small SD (1.5 m at end of July 1984). Turbid alpine rivers (Arve, Rhône) cluster (M) towards the equal radiance point E, and chalky bottom sediments more or less covered with aquatic macrophytes (SAV) plot at B. The remaining water bodies are located between these attraction points, and some of them plot along well-defined loci. They are:

1) *Pelagic zone – total lake – chalky bottom.* As already mentioned, the whole lake includes signals from shallow-water banks. In most cases, they consist of white lacustrine chalk more or less covered with SAV, resulting in the intermediate position of B between C and M. This first trend type (Fig. 4), however short, consistently points towards B.
2) *Pelagic zone – total lake – sandy bottom.* In the large subalpine lac Léman, shallows are sandy (Vernet et al. 1972) and the SAV cover is dense (Lachavanne and Wattenhoffer 1975). They plot along a curvilinear locus among 'normal' water bodies from which they cannot be discriminated. This is in agreement with Ackleson and Klemas'(1987) results in Chesapeake Bay, where the signature from dense SAV cannot be isolated from that of deep water.
3) *Clear water – turbid water (mineral turbidity).* The relatively clear water of Léman (1-2 g/m$^3$ in Summer, Jaquet et al. 1983) empties into the Rhône river in Geneva, which receives the highly turbid alpine Arve river (>100 g/m$^3$sm). The mixed waters are then retained behind Verbois dam (Fig. 1). The locus is curvilinear, going from lac Léman – mixture Rhône+Arve – Arve with increasing turbidity. It is similar in shape and orientation to loci shown in Munday et al. (1979) and Alfoldi and Munday (1978). It points towards the land target (T) and the iso-radiance point E.

*3.2.2. Interpretation*

Bukata et al. (1983) have generated subsurface irradiance spectra for lake Ontario modelled as a 4-component

**Table 3 - MEAN DIGITAL REFLECTANCE FOR TM BANDS 1, 2, 3, 4, 6 AND CHROMATICITY VALUES**

| Name | No | CH1M | CH2M | CH3M | CH4M | CH6M | X | Y | Z |
|---|---|---|---|---|---|---|---|---|---|
| CHALAIN_0 | 1 | 92.14 | 35.77 | 19.17 | 12.14 | 127.16 | 0.447 | 0.419 | 0.133 |
| CHALAIN_5 | 2 | 90.65 | 34.51 | 17.43 | 10.09 | 126.26 | 0.457 | 0.419 | 0.125 |
| NARLAY_P | 3 | 60.10 | 18.89 | 12.92 | 9.73 | 124.39 | 0.492 | 0.362 | 0.146 |
| GD_MACLU_P | 4 | 57.83 | 18.10 | 12.58 | 9.14 | 125.13 | 0.493 | 0.360 | 0.147 |
| LA_MOTTE_P | 6 | 64.10 | 22.25 | 13.53 | 9.44 | 124.46 | 0.473 | 0.389 | 0.138 |
| CHAMBLY_NP | 7 | 65.52 | 21.72 | 14.23 | 10.58 | 127.20 | 0.480 | 0.375 | 0.145 |
| CHAMBLY_SP | 8 | 66.92 | 23.64 | 14.84 | 10.56 | 126.13 | 0.465 | 0.390 | 0.144 |
| BONLIEU_P | 9 | 63.46 | 22.69 | 13.62 | 9.16 | 124.48 | 0.466 | 0.395 | 0.139 |
| MOTTE_1 | 9 | 84.07 | 41.57 | 30.00 | 14.79 | 127.21 | 0.366 | 0.440 | 0.194 |
| ABBAYE_P | 10 | 57.25 | 18.46 | 13.11 | 9.45 | 123.85 | 0.483 | 0.364 | 0.153 |
| CLAIRV_NO | 11 | 94.14 | 39.74 | 25.88 | 13.91 | 128.25 | 0.412 | 0.422 | 0.166 |
| CLAIRV_NP | 12 | 87.31 | 34.22 | 19.10 | 10.51 | 126.78 | 0.443 | 0.418 | 0.139 |
| CLAIRV_SP | 13 | 79.60 | 29.05 | 17.42 | 11.02 | 126.79 | 0.458 | 0.400 | 0.142 |
| ROUSSES_P | 14 | 57.97 | 19.24 | 13.66 | 9.96 | 121.39 | 0.475 | 0.370 | 0.155 |
| JOUX_0 | 15 | 82.05 | 45.73 | 29.52 | 11.76 | 122.42 | 0.345 | 0.470 | 0.185 |
| JOUX_P | 16 | 82.36 | 46.08 | 29.33 | 11.18 | 121.44 | 0.345 | 0.472 | 0.183 |
| TER | 17 | 61.60 | 22.87 | 17.27 | 12.60 | 129.13 | 0.438 | 0.386 | 0.176 |
| BRENET_P | 24 | 78.38 | 42.08 | 28.92 | 14.13 | 123.41 | 0.350 | 0.458 | 0.192 |
| BRENET_0 | 25 | 78.48 | 42.01 | 29.15 | 15.78 | 124.40 | 0.350 | 0.457 | 0.193 |
| ANNECY_0 | 26 | 76.40 | 25.74 | 16.39 | 9.99 | 124.38 | 0.475 | 0.381 | 0.144 |
| ANNECY_P | 27 | 75.66 | 25.01 | 15.93 | 9.78 | 123.88 | 0.480 | 0.377 | 0.142 |
| GIROTTE_P | 28 | 131.52 | 62.75 | 46.35 | 12.99 | 106.07 | 0.371 | 0.433 | 0.197 |
| GITTAZ_P | 29 | 69.53 | 22.23 | 14.55 | 10.84 | 109.64 | 0.488 | 0.369 | 0.143 |
| ROSELEND_0 | 30 | 68.90 | 26.06 | 16.16 | 10.24 | 111.14 | 0.448 | 0.404 | 0.148 |
| ROSELEND_P | 31 | 68.75 | 26.08 | 16.16 | 10.02 | 109.69 | 0.447 | 0.405 | 0.148 |
| GUERIN_P | 32 | 69.80 | 26.67 | 18.20 | 10.95 | 106.10 | 0.437 | 0.399 | 0.163 |
| BOURGET_0 | 33 | 79.32 | 30.40 | 17.77 | 9.66 | 127.22 | 0.446 | 0.411 | 0.143 |
| BOURGET_P | 34 | 79.77 | 30.67 | 17.66 | 9.35 | 127.14 | 0.447 | 0.413 | 0.141 |
| AIGUEBEL_0 | 35 | 81.32 | 29.72 | 17.52 | 11.20 | 128.39 | 0.458 | 0.401 | 0.140 |
| AIGUEBEL_P | 36 | 80.40 | 28.55 | 16.08 | 9.32 | 127.75 | 0.469 | 0.399 | 0.132 |
| VOUGLANS_S | 37 | 93.89 | 38.76 | 20.81 | 10.05 | 126.85 | 0.431 | 0.431 | 0.138 |
| VOUGLANS_M | 38 | 87.35 | 35.77 | 19.90 | 10.27 | 125.86 | 0.432 | 0.427 | 0.141 |
| VOUGLANS_N | 39 | 76.91 | 32.44 | 19.79 | 10.18 | 128.06 | 0.419 | 0.426 | 0.155 |
| CONDES_P | 40 | 66.05 | 24.11 | 16.48 | 10.15 | 126.65 | 0.450 | 0.391 | 0.159 |
| NANTUA_0 | 41 | 66.57 | 23.67 | 16.30 | 10.83 | 126.34 | 0.456 | 0.385 | 0.158 |
| NANTUA_P | 42 | 66.89 | 23.78 | 16.35 | 10.56 | 125.03 | 0.456 | 0.385 | 0.158 |
| SYLANS_P | 43 | 77.33 | 32.72 | 19.14 | 10.30 | 127.04 | 0.421 | 0.429 | 0.150 |
| REMORAY_CR | 44 | 85.05 | 43.53 | 34.54 | 12.48 | 125.99 | 0.350 | 0.437 | 0.213 |
| REMORAY_0 | 45 | 69.75 | 27.93 | 19.70 | 13.39 | 124.87 | 0.422 | 0.405 | 0.172 |
| REMORAY_P | 46 | 65.53 | 23.19 | 14.67 | 9.94 | 123.29 | 0.464 | 0.390 | 0.145 |
| GRUYERES_P | 47 | 83.43 | 39.18 | 26.11 | 11.97 | 124.27 | 0.384 | 0.438 | 0.177 |
| MONTSALVEN | 48 | 63.85 | 22.05 | 15.87 | 12.18 | 118.36 | 0.461 | 0.377 | 0.162 |
| SARINE_P | 49 | 78.11 | 31.38 | 20.20 | 12.75 | 113.88 | 0.427 | 0.413 | 0.160 |
| BRET_P | 52 | 67.46 | 26.26 | 18.10 | 11.85 | 126.37 | 0.432 | 0.402 | 0.166 |
| BRET_0 | 53 | 67.71 | 26.45 | 18.74 | 15.13 | 127.33 | 0.429 | 0.401 | 0.171 |
| EMOSSON | 54 | 101.57 | 43.65 | 32.02 | 10.77 | 109.50 | 0.398 | 0.415 | 0.187 |
| SALANFE | 55 | 83.44 | 32.54 | 20.76 | 9.84 | 110.75 | 0.435 | 0.408 | 0.156 |
| MONTRION_P | 56 | 61.68 | 21.60 | 13.36 | 9.91 | 121.23 | 0.470 | 0.389 | 0.141 |
| ANTERNE_P | 57 | 62.55 | 20.66 | 13.79 | 8.62 | 109.00 | 0.480 | 0.373 | 0.147 |
| NOIR | 58 | 54.92 | 18.19 | 13.77 | 18.12 | 118.96 | 0.471 | 0.365 | 0.164 |
| DIVONNE_P | 59 | 70.32 | 25.68 | 17.65 | 11.67 | 130.01 | 0.449 | 0.391 | 0.161 |
| VERBOIS | 60 | 90.78 | 36.68 | 26.08 | 12.93 | 126.29 | 0.417 | 0.407 | 0.176 |
| MACHILLY_P | 61 | 73.22 | 30.61 | 24.94 | 18.03 | 132.69 | 0.399 | 0.401 | 0.200 |
| LEMAN_P | 62 | 66.36 | 21.20 | 14.49 | 8.57 | 124.59 | 0.486 | 0.366 | 0.148 |
| LEMAN_VIDY | 63 | 68.40 | 21.90 | 14.79 | 8.53 | 123.25 | 0.486 | 0.367 | 0.147 |
| LEMAN_ROLL | 64 | 67.61 | 21.44 | 15.00 | 8.69 | 124.19 | 0.486 | 0.363 | 0.151 |
| LEMAN_DRAN | 65 | 66.31 | 20.97 | 14.23 | 8.25 | 125.03 | 0.489 | 0.364 | 0.146 |
| LEMAN_EVIA | 66 | 65.34 | 20.89 | 14.09 | 8.39 | 125.02 | 0.487 | 0.367 | 0.146 |
| LEMAN_LOCU | 67 | 64.29 | 20.64 | 13.94 | 8.60 | 123.86 | 0.486 | 0.367 | 0.146 |
| LEMAN_RHON | 68 | 66.12 | 21.50 | 14.54 | 9.01 | 124.01 | 0.482 | 0.370 | 0.148 |
| LEMAN_VILL | 69 | 65.93 | 21.34 | 14.30 | 9.43 | 124.26 | 0.484 | 0.369 | 0.146 |
| ARVE_MIN | 70 | 99.00 | 46.00 | 44.00 | 27.00 | 132.00 | 0.357 | 0.404 | 0.240 |
| ARVE_CONTA | 71 | 102.00 | 45.00 | 43.00 | 20.00 | 126.00 | 0.369 | 0.396 | 0.235 |
| RHONEVS_A | 72 | 102.00 | 48.00 | 43.00 | 22.00 | 117.00 | 0.359 | 0.412 | 0.229 |
| RHONEVS_B | 73 | 102.00 | 47.00 | 46.00 | 21.00 | 117.00 | 0.357 | 0.400 | 0.243 |
| RHONE_GEA | 74 | 81.00 | 33.00 | 22.00 | 14.00 | 130.00 | 0.421 | 0.413 | 0.166 |
| TANNAY_P | 77 | 61.18 | 20.64 | 13.69 | 10.67 | 118.67 | 0.475 | 0.378 | 0.147 |
| HONGRIN_P | 78 | 63.56 | 22.17 | 15.21 | 11.23 | 117.51 | 0.463 | 0.382 | 0.156 |
| GENIN | 79 | 63.89 | 23.95 | 15.53 | 10.32 | 127.32 | 0.447 | 0.399 | 0.153 |
| PALEXPO | 80 | 181.24 | 93.86 | 115.29 | 98.95 | 171.43 | 0.308 | 0.392 | 0.301 |
| RHONE_BUTI | 81 | 85.14 | 35.32 | 26.23 | 23.68 | 134.41 | 0.407 | 0.408 | 0.185 |
| RADE_GE | 82 | 68.47 | 23.42 | 17.69 | 9.88 | 125.84 | 0.459 | 0.372 | 0.169 |
| ARVE_BATIE | 83 | 100.59 | 45.09 | 42.73 | 23.68 | 131.18 | 0.366 | 0.399 | 0.235 |
| LEM_VENG | 84 | 74.34 | 29.44 | 19.36 | 11.24 | 128.64 | 0.430 | 0.409 | 0.161 |
| LEM_BIT | 85 | 72.60 | 26.33 | 17.67 | 10.08 | 126.38 | 0.452 | 0.391 | 0.157 |
| LEM_TRAVER | 86 | 71.59 | 26.22 | 17.50 | 9.56 | 125.72 | 0.450 | 0.393 | 0.157 |
| LEM_BABYPL | 87 | 69.42 | 25.52 | 17.07 | 9.42 | 124.57 | 0.449 | 0.394 | 0.157 |
| LEM_NAUTIQ | 88 | 70.79 | 25.97 | 16.69 | 9.97 | 126.17 | 0.453 | 0.396 | 0.151 |
| LEM_GRANG1 | 89 | 70.16 | 26.91 | 17.81 | 10.09 | 122.93 | 0.439 | 0.402 | 0.159 |
| LEM_GRAN2 | 90 | 74.14 | 30.13 | 21.33 | 10.64 | 123.77 | 0.418 | 0.408 | 0.174 |
| LEM_GRAN3 | 91 | 73.25 | 29.46 | 20.81 | 12.89 | 124.94 | 0.421 | 0.406 | 0.173 |
| CLAIRV_1 | 93 | 108.86 | 54.86 | 44.14 | 27.33 | 130.00 | 0.352 | 0.433 | 0.215 |
| CLAIRV_2 | 94 | 96.12 | 39.97 | 22.79 | 11.27 | 128.70 | 0.425 | 0.428 | 0.146 |
| CLAIRV_3 | 95 | 91.14 | 36.60 | 20.20 | 11.06 | 126.80 | 0.437 | 0.424 | 0.139 |

water mass [water, chlorophyll (ch), mineral suspensoids (sm) and dissolved organic carbon (doc)]. They also computed chromaticity coordinates (blue, green, red) for water with doc=0 or 2 g/m$^3$, ch between 0.05-20 mg/m$^3$ and sm between 0-20 g/m$^3$ (their Figs. 9 and 10): chromaticity loci for ch and sm are practically coincident up to concentrations of 3 mg/m$^3$ and 1 g/m$^3$, respectively. Beyond, they separate to form a loop with maximum opening (0.02 $Y$ units) for ch=20 mg/m$^3$ and sm=20 g/m$^3$. The loci in Figure 4. form a pattern quite similar, with even a better separation (0.07 units) between the chlorophyll AP and the alpine rivers AP, which is pulled towards desaturation point E. This favourable feature stems from the high sm concentration in Rhône and Arve rivers ($\geqslant$100 g/m$^3$).
Whilst $X$ chromaticity is inversely related to total suspensoid concentration, $Y$ ('greenness') allows a certain discrimination between the AP B, C and M.

The variable curvature of the chlorophyll and sm loci is probably due to the combined influence of suspensoids on hue and saturation: the colourless mineral suspensions mainly act as desaturating agents with little influence on hue, whereas coloured plant pigments logically induce a larger hue shift. Work is in progress to test this hypothesis. The straightness of type 1 trend is due to a simple mixture between the colour of deep, more saturated water and that of AP B.

It should also be noted that, since the water bodies are all located below point E on Figure 4a, a lowering of saturation corresponds to an increase along the $Z$ axis.

Another feature of interest visible on these diagrams is the spread along the $Y$ axis (or towards green) between green-blue lakes (Léman, La Motte) and greener ones (Chalain): this could be an effect of qualitative rather

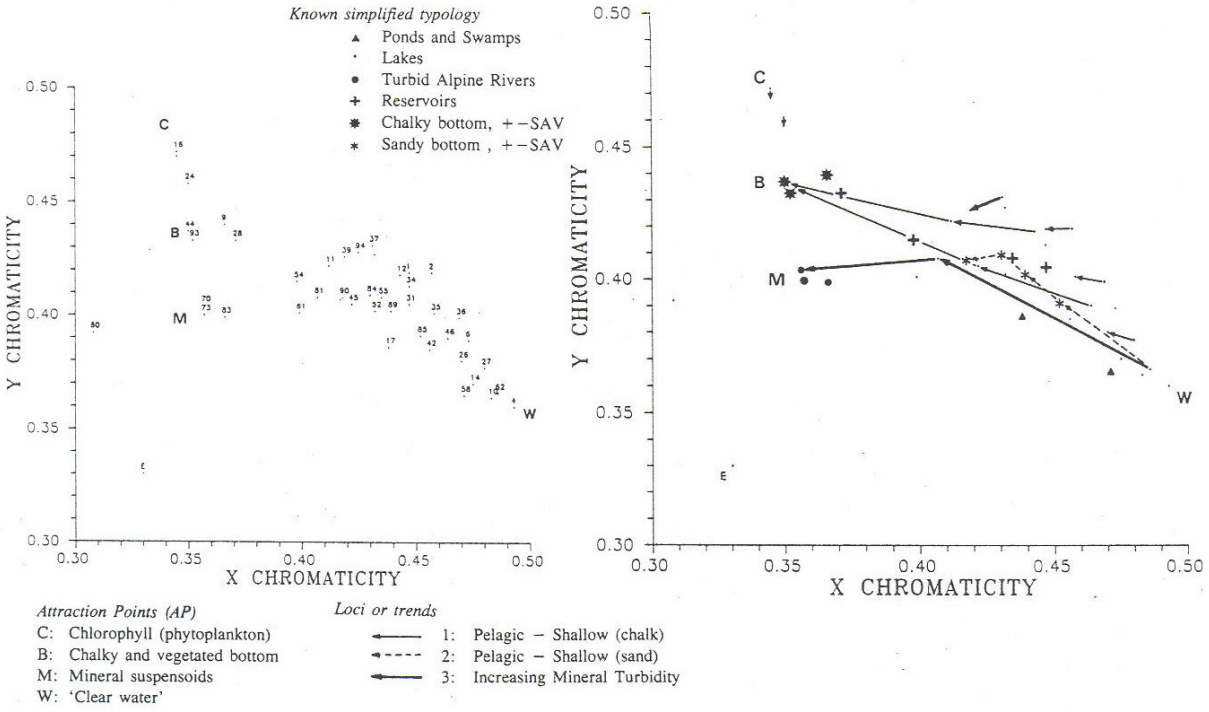


*Figure 4a. Location of selected water targets in chromaticity space with typology and trends.*

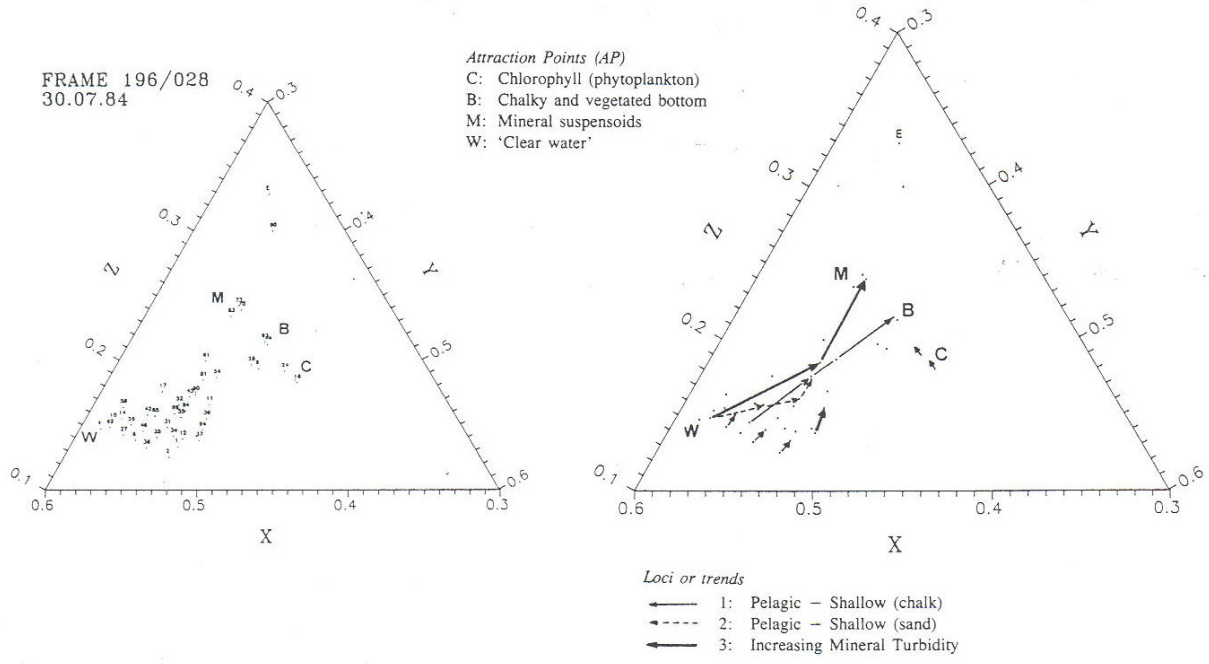


*Figure 4b. Location of selected water targets in triangular chromaticity space with trends.*

than quantitative changes in pigment (different phytoplanctonic species).

### 3.3. Four-band classification based on intensity

The information contained in the TM bands 1-4 was condensed by principal component analysis (PC) (Table 5). The results confirm the features of the correlation coefficient matrix (Table 4): the first 3 bands are highly correlated, giving a PC allowing for more than 90% of the variance. The second PC expresses the influence of NIR1 and red bands.

A cluster analysis was performed on the PC's scores, resulting in the diagram of Figure 5. The groups are

**Table 4 - CORRELATION BETWEEN TM BANDS FOR SELECTED WATER BODIES (PELAGIC ZONE).N = 45**

| Band | 1 | 2 | 3 | 4 | 6 |
|---|---|---|---|---|---|
| 1 | | .94 | .86 | .31 | -.11 |
| 2 | | | .93 | .34 | -.09 |
| 3 | | | | .51 | -.03 |
| 4 | | | | | .31 |

**Table 5 - PRINCIPAL COMPONENT ANALYSIS OF SELECTED WATERBODIES (PELAGIC ZONE) BASED ON DN's OF TM BANDS 1, 2, 3 AND 4. N = 45**

| PC | 1 | 2 | 3 | 4 |
|---|---|---|---|---|
| Variance % | 91.3 | 5.4 | 2.6 | 0.7 |
| Cum. var. | 91.3 | 96.7 | 99.3 | 100.0 |
| Eigenvectors | | | | |
| Band 1 | .79 | -.39 | -.46 | -.15 |
| Band 2 | .49 | .11 | .53 | .68 |
| Band 3 | .37 | .52 | .40 | -.66 |
| Band 4 | .09 | .75 | -.59 | .28 |

represented in the PC1−PC2 space, and are discriminated essentially through intensities in bands 1, 2 and 3 (the vertical scale is blown up for clarity). Some of the trends defined above (3.2.1) are also shown. Although they are not consistent along PC1, the turbidity trends are proportional to PC2, which confirms the well-known correlation between turbidity and NIR1.

Ten groups are plotted on Figure 5, part of which can be related to the colour analysis results. Group 1 corresponds to 'dark lakes', with possibly some influence from peaty bottoms shown by relatively high values in PC2. Gr5 includes shallow, rather turbid lakes used for recreation and fishing (bottom resuspension?), and Gr6 productive 'green' lakes Joux and Brenet. Turbid rivers fall in Gr8 and 9, and alpine reservoirs in Gr7 and 10.

The relative difficulty in interpreting such a classification comes from the fact that intensity, as opposed to hue and saturation, often depends on transient, parasitic phenomena such as waves or white caps.

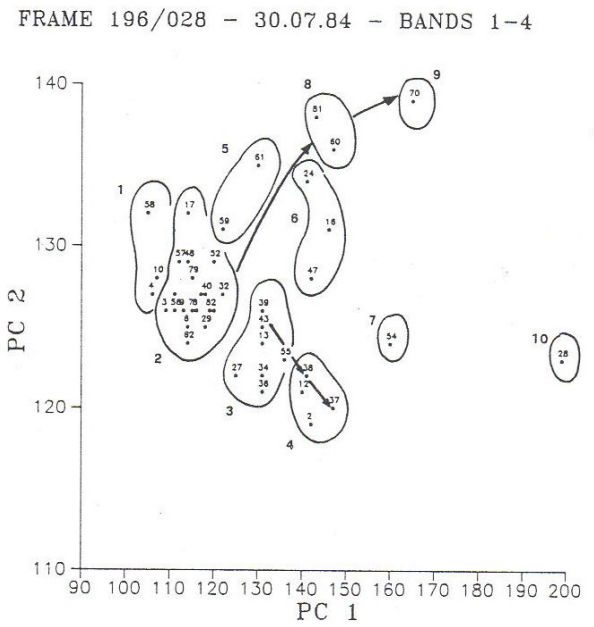


*Figure 5. Classification of water bodies (Pelagic) by Cluster analysis in the two first principal components space. Group limits hand-drawn.*

## 4. Discussion and Conclusions

The ground information available on the water bodies, not collected on the day of overpass, is very heterogeneous. Whereas some lakes such as Léman (Cipel 1984), Joux, Bourget and Jura lakes (Verneaux et al. 1987) are monitored more or less regularly, very little is known about the others (Table 2, column 6).

The notion of trophic state is a widely used, 'better-than-nothing' integrative descriptor for lakes. Discussing the merits of this notion is beyond our scope here. Suffice it to say that 'trophy' can be estimated via SD, total phosphorus or chlorophyll concentration (OECD 1982), and also from satellite data (Scarpace et al. 1979).

Chromaticity analysis, as shown on Figure 4 and restricted to pelagic data, allows a discrimination between oligo-mesotrophic lakes located around W (Maclu, La Motte, Léman, Annecy), meso-eutrophic (Bourget) and eutrophic ones (C: Joux, Brenet), following a trend of increasing pigment content. Moreover, the trend towards E separates water bodies chiefly on mineral turbidity, culminating at M (very turbid waters).

It is probable that water colour contains more information on other limnological parameters. For instance, within-lake hue and saturation heterogeneities are visible on the images, combined with thermal contrasts (TM band 6). This could help estimate spatial variability in lakes, almost impossible to measure with conventional methods.

In order to fully exploit colour information, the following should be undertaken:

1) *Ground colour measurements* conducted in situ and also on the organic and mineral suspensoids, so as to assess their bearing on hue and saturation.
2) Further *simulation of irradiance spectra* using a refined version of Bukata et al.'s (1983) model. In particular, the influence of phytoplankton type (pigment, size) should be estimated, as well as that of mineral particles (quartz, clay, autochtonous $CaCO_3$, Galat and Jacobsen 1985).
3) Application of *atmospheric correction* to allow for multidate colour analysis and a generalisation of the relationships found in this preliminary study.

At this stage, we can conclude that an excellent ground resolution and the presence of a 'blue' band make Landsat TM a valuable tool for the study of inland waters – superior in that to the much used MSS.

## Acknowledgements

This report is a product of a continuing joint venture between UNEP-GRID and University of Geneva. The assistance and encouragments of D.W. Mooneyhan, director, and L. McGregor, both with GRID-P, are gratefully acknowledged, as well as that of J. Charollais, director of the Geology Department.

## References

Ackelson S.G. and Klemas V., 1987. Remote Sensing of Submerged Aquatic Vegetation in Lower Chesapeake Bay: A Comparison of Landsat MSS to TM Imagery. *Remote Sens. Envir.* 22: 235-238.

Alföldi T.T. and Munday J.C., 1978. Water Quality Analysis by Digital Chromaticity Mapping of Landsat Data. *Can. Jour. Remote Sens.* 4(2): 108-126.

Blackwell R.J. and Boland D.H., 1976. The Trophic Classification of Lakes Using ERTS Multispectral Scanner Data. *Proc. Amer. Soc. Photogram. 41st Ann. Meet.*, Falls Church, 393-414.

Bukata R.P., Bruton J.E. and Jerome J.H., 1983. Use of Chromaticity in Remote Measurements of Water Quality. *Remote Sens. Envir.* 13: 161-177.

Cipel, 1984. *Le Léman, synthèse 1957–1982.* Comm. Internat. Protection du Léman, Lausanne, 650 p.

Delebecque A., 1898. *Les lacs français.* Béranger, Paris, 435 p.

Galat D.L. and Jacobsen R.L. 1975. Recurrent aragonite precipitation in saline-alkaline Pyramid Lake, Nevada. *Arch. Hydrobiol.* 105(2): 137-159.

Gordon H.R. and McCluney W.R., 1975. Estimation of the Depth of Sunlight Penetration in the Sea for Remote Sensing. *Applied Optics* 14(2): 413-416.

Jaquet J.-M., Favarger P.-Y., Peter A. and Vernet J.-P., 1983. *Premières données sur la matière en suspension dans le Léman.* Internal Report, Institut Forel, University of Geneva, 83 p.

Jaquet J.-M., 1987. *Remote Sensing Evaluation of Water Quality in the Gulf of Nicoya (Costa Rica).* Annex to FAO Fisheries Technical Paper 287: 35-50.

Jerlov N.G., 1976. *Marine Optics.* Elsevier Publ., Amsterdam, 231 p.

Lachavanne J.-B. and Wattenhoffer R., 1975. *Les Macrophytes du Léman.* Comm. Internat. Protection du Léman, Lausanne, 147 p.

Lathrop R.G. and Lillesand T.M., 1986. Use of Thematic Mapper Data to Assess Water Quality in Green Bay and Central Lake Michigan. *Photogr. Engin. Rem. Sens.* 52(5): 671-680.

Lathrop R.G. and Lillesand T.M., 1987. Calibration of Thematic Mapper Thermal Data for Water Surface Temperature Mapping: Case Study on the Great Lakes. *Remote. Sens. Envir.* 22: 297-307.

Lemoalle J., 1979. Application des données Landsat à l'estimation de la production du phytoplancton dans le lac Tchad. *Cah. ORSTOM, sér. Hydrobiol.*, 13(1-2): 35-46.

Lindell L.T., Steinvall O., Jonsson M. and Claesson T., 1985. Mapping of coastal-water turbidity using Landsat imagery. *Int. J. Remote Sensing* 6(5): 629-642.

Lillesand T.M., Johnson W.L., Deuell R.L., Lindstrom O.M. and Meisner D.E., 1983. Use of Landsat Data to Predict the Trophic State of Minnesota Lakes. *Photogr. Engin. Rem. Sens.* 49(2): 219-229.

McGarrigle M.L. and Reardon B.C., 1986. *National Survey of Lakes by Remote Sensing.* Preliminary report, WR/L13, An Foras Forbartha, Dublin, 31 p.

Munday J.C., Alföldi T.T. and Amos C.L., 1979. Verification and Application of a System for Automated Multidate Landsat Measurement of Suspended Sediment. *Satell. Hydrol., Amer. Water Res. Assoc.*, June 1979, 622-640.

OCDE, 1982. *Eutrophication of waters: monitoring, assessment and control.* OCDE, Paris, 154 p.

Piech K.R. and Walker J.E., 1971. Aerial Color Analyses of Water Quality. *Jour. Survey. Mapp. Div., Amer. Soc. Civil Engin.*, SU 2, Nov. 71: 185-197.

Piech K.R., Schott J.R. and Stewart K.M., 1978. The Blue-to-Green Reflectance Ratio and Lake Water Quality. *Photogr. Engin. Rem. Sens.* 44(10): 1303-1310.

Poros D. and Peterson C.J., 1985. Methods for Destriping Landsat Thematic Mapper Images - A Feasibility Study for an Online Destriping Process in the Thematic Mapper Image Processing System (TIPS). *Photogr. Engin. Rem. Sens.* 51(9): 1371-1378.

Rochon G., 1975. *Etude méthodologique de l'évolution et de la classification des lacs par satellite.* CRE-75/06, Minist. Richesses Nat. du Québec, 90 p.

Scarpace F.L., Holmquist K.W. and Fisher L.T., 1979. Landsat Analysis of Lake Quality. *Photogr. Engin. Rem. Sens.* 45(5): 623-633.

Scherz J.P. and Van Domelen J.F., 1974. Water Quality Indicators Obtainable from Aircraft and Landsat Images and their Use in Classifying Lakes. *10th ERIM Symp.*: 447-460.

Shimoda H., Etaya M., Sakata T., Goda L. and Stelczer K., 1984. Water Quality Monitoring of Lake Balaton using Landsat MSS Data. *18th ERIM Symp.*: 565-574.

Slater P.N., Biggar S.F., Holm R.G., Jackson R.D., Mao Y., Moran M.S., Palmer J.H. and Yuan B., 1987. Reflectance- and Radiance-Based Methods for the In-Flight Absolute Calibration of Multispectral Sensors. *Rem. Sensing Envir.* 22: 11-37.

Smith A.Y. and Addington J.D., 1978. Water Quality Monitoring of Lake Mead: a Practical Look at the Difficulties Encountered in the Application of Remotely Sensed Data to Analysis of Temporal Change. *5th Canad. Symp. on Remote Sens.* 174-186.

Smith R.C., Tyler J.E. and Goldman C.R., 1973. Optical properties and color of lake Tahoe and Crater lake. *Limno. Oceano.* 18(2): 189-199.

Tassan S., 1984. *Evaluation of the potential of the thematic mapper for chlorophyll and suspended matter determination in sea water.* Joint Research Centre, Ispra, Internal Rept., 21-25.

Verneaux J., Remy F., Vidonne A. and Guyard A., 1987. Caractères généraux des sédiments de 10 lacs jurassiens. *Sciences de l'Eau,* 6: 107-128.

Vernet J.-P., Thomas R.L., Jaquet J.-M. and Friedli R., 1972. Texture of the Sediments of the Petit Lac (Western Lake Geneva). *Eclogae Geol. Helv.* 65(3): 591-610.

Wezernak C.T., Tanis F.J. and Bajza C.A., 1976. Trophic State Analysis of Inland Lakes. *Remote Sens. Envir.* 5: 147-165.